공학석사학위논문

사각 기포탑 혼합 및 수력학적 특성에 관한 실험적 연구

Experimental Investigation on Different Hydrodynamics and Mixing Characteristics for Rectangular Bubble Column

2017 년 02월

서울개학교 대학원

기계항공공학부

Islam MD Zahidul

Experimental Investigation on Different Hydrodynamics and Mixing Characteristics for Rectangular Bubble Column

지도교수 박형민

이 논문을 공학석사학위논문으로 제출함

2016 년 10월

서울대학교 대학원

기계항공공학과

자히둘

자히둘의 석사학위논문을 인준함

2016 년 12월

위 원 장 최해천 (인)

부 위 원 장 박형민 (인)

위 원 황원태 (인)

Experimental Investigation on Different Hydrodynamics and Mixing Characteristics for Rectangular Bubble Column

Islam MD Zahidul

Department of Mechanical and Aerospace Engineering

Seoul National University

Abstract

Mixing and transport processes are the key issues in studying two-phase bubbly flow in a bubble column. Especially, the bubble-induced liquid phase mixing is a complex function of void fraction distribution, gas phase velocity and so on. To study the characteristics of the mixing induced by the bubbles, we have designed a rectangular bubble column where the mean void fractions ranging from 0.006 to 0.075%. High-speed shadowgraphy technique is used to measure the different gas phase properties such as bubble size, void fraction, and bubble velocity. To measure the mixing, on the other hand, we have used a direct visualization method with low diffusive buoyant dye. The results reveal both qualitative and quantitative measurements.

Key Words: bubbly flow (기포류유동), bubble column(기포탑), bubble distribution (기포분포), dye visualization(염료가시화) mixing (혼합).

Student number : 2015-22131

Contents

List of Figures

Figure 4.7: Concentration profile for green dye (a) 1x2, (b) 2x2, (c) 4x4 for a given time of t= 6.5s.

Figure 4.8: Relation between mixing time and volume void fraction

Nomenclature

A : 기호설명(m/s)

AR : 기포의 가로세로비

d_B : 기포의 지름 (mm)

Ro : 형상인자 (shape factor)

u : 기포의 자유 상승속도(mm/s)

x : 유동방향에 수직한 방향

y : 유동방향

<α> : 체적 평균 기포분율

Chapter 01

Introduction

Bubbly flows are used in many industrial applications such as refining, chemical, petrochemical & waste water management industries. Bubbly flows can be seen in many gas-liquid contacting apparatus such as aerated stirred reactors, bubble columns, air-lift columns (Laurent and carpenter, 1974). In bubble column the rising motion of the injected bubbles produces a liquid fluctuation which can mix the chemical species without requiring any extra mechanical devices and agitation.

Bubble injection into a liquid of homogenous flow generates entrainment of liquid from the column and induces large scale buoyancy-driven circulation in the surrounding liquid. This physics is mainly responsible to create the upward momentum of the liquid in the plume due to buoyancy, since the upward bubbles have relative movements and entrain liquid in their wakes (J. Rensen, V. Roig, 2001). Freedman and Davidson (1969) were the first who raised up this issue of circulation in bubble columns in which they have developed a liquid circulation model known as the "gulf stream" or cooling tower model. In their study they proposed that the liquid circulation consists of two adjacent vortex cells with liquid flowing upward in the center of the bubble and downward along the walls of the columns at later. Joshi and Sharma (1979), Chen et al. (1989) experimentally investigated this "cooling tower" in terms of different aspect ratio, void fraction, and superficial gas velocity.

In Bubble columns, the bubbles usually injects from the bottom of the column into a homogenous liquid as a result bubbles induces entrainment of liquid from the column and generates large scale buoyancy-driven circulation in the surrounding

liquid. Since bubbles have relative upward movement and entrain liquid present in their wake so the basic mechanism which is responsible for the upward liquid momentum is buoyancy.

In literature it can be found that various studies have done on bubble plume experiments where maximum studies concerned very large scale bubble plumes for environmental applications as well as chemical processing applications has also scales into a small scale (Milgram, 1983; Leitch and Baines, 1989; Alam and Arakeri, 1993; Becker et al,. 1994; Iguchi et al., 1995; Iguchi et al., 1997; Delnoij et al., 1997;). Some of the research study also reported oscillation of the uprising bubble plume in the stationary liquid. In general this oscillation has to found depends on various hydrodynamics properties like bubble phase velocity, aspect ratio etc. (Dlnoij et al., 1997, Buwa and Ranade., 2002; Rensen and Roig, 2001, Diaz et al., 2006;2007, R.K. Upadhya et al 2013) However only a few studies have shown relation between the mixing times with the bubble column hydrodynamics.

On the other hand several researchers have performed their study to reveal the mixing characteristics in terms of Bubble Induced turbulence and Shear Induced turbulence. In chemical industry or process plant bubbly flows are used to mix the flow and increase the efficiency of the reactions (M. Simiano et al 2006). Though previous literature study were confined their study in a confined bubble column but here in our study we have relatively non-confined bubble column setup has used. To predict the mixing time in a passive scalar form is still inadequate in number in present literature study. To predict scalar form mixing time with the different operating conditions we have introduced direct visualization method using an almost buoyant color dye. Almeras et al. 2016 has showed and modeled the mixing time with the gas volume fraction. We found interest to check our result with Almeras as an initial approach to our further research. Interestingly in Almeras approach the gas volume fraction was higher than our range but our calculation also get fit with the Almeras model. In our section three we will describe it in more.

In our present study we have performed our study in a flat rectangular bubble

column which satisfy several of our interest. First we have used image processing technique to reveal our study on the different hydrodynamics and mixing characteristics, to perform this a flat 2D rectangular bubble column is appropriate enough (R.K. Upadhya et al. 2013). Also for qualitative approach and visualization for the mixing time 2D flat rectangular column have been used by several research group in previous study.

Before modeling the mixing characteristics in a bubble column it is crucial to investigate and model the complex hydrodynamics of the bubble column as the characteristics of mixing is a complex function of different hydrodynamics properties of the bubble column. So in this work we will have two sections for the discussions, the first one will be the characterizing of the different hydrodynamics of the bubble column and the second one will be the mixing characteristics depends on the hydrodynamics of the bubble column. To reveal the hydrodynamics of the bubble column we have used the high-speed shadowgraphy technique to visualize the bubbly flow and different gas phase properties such as void fraction, bubble size & bubble velocity. For revealing the mixing time in the bubble column depends on different hydrodynamics we have used low diffusive buoyant dye. For shadowgraphy, we have used an in-house image processing technique which will be also discussed later.

In our present study we have shown the effect of increasing the gas volume fraction on the bubble phase velocity distribution, bubble size distribution, PDF of several hydrodynamics of the bubble column. Finally we have characterized the mixing time with the gas volume void fraction.

The objective of this study is to provide the relation of the different hydrodynamics properties and then provide the mixing time based on the different hydrodynamics properties. Our void fraction ranging from 0.006 to 0.075%. In our study we have considered mixing induced by the bubbles in the absence of any liquid main flow and shear induced turbulence. The detail description of the experimental setup and method will be provided in section two. And afterwards the results will be described.

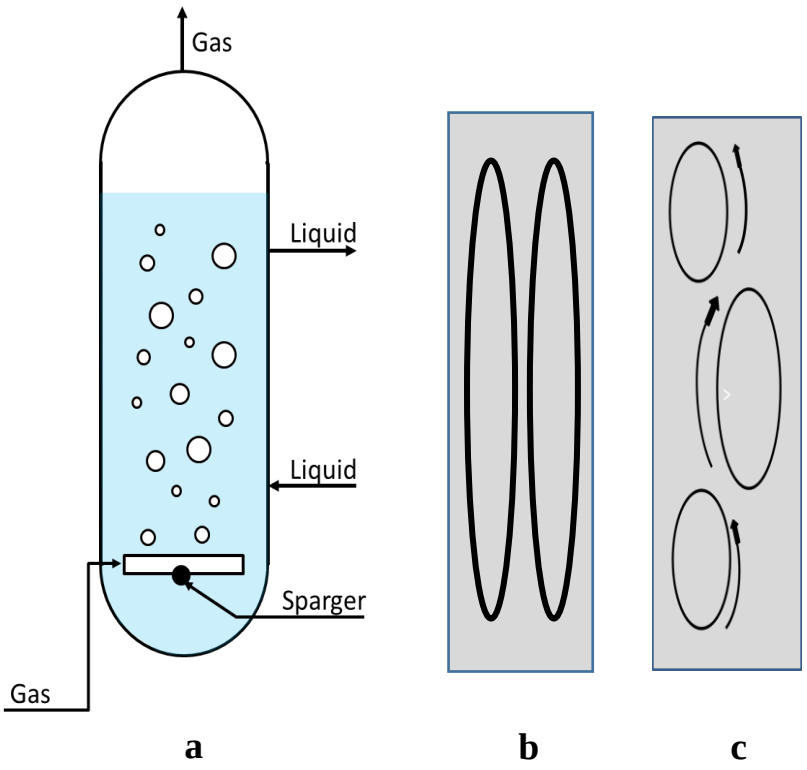

Figure 1: a) A simple schematic of Bubble Column system. b) Time averaged flow structure in a bubble column; c) unsteady flow structure in a bubble column.

Chapter 2

Experimental setup

The experiments have conducted in the square shaped acrylic made water tank of which 150X150X500 mm^3 as shown in figure 2.1 (a). The tank has filled with water upto a height of 450mm. The reason to choose this height is because in the several researchers have mentioned that we can neglect the effect of height on the hydrodynamics of the bubble column when the aspect ratio maintained to 3 or above (N. Kantarci et al. 2005). The air bubbles come from an air compressor through a regulator and then it passed through a solenoid valve and small scale regulator and finally through stainless steel injector. The injectors are arranged at the middle of 8X8 square array of total 64 injectors. Though in our experiments we have used upto 16 injectors. The pitch was 8mm and inner diameter of the nozzle was 0.84mm. The LED array with 532nm of wavelength has placed at the back of the tank so that the bubble shadow can be captured by the high speed camera.

In our experimental condition we have used three different injectors setup for varying our gas volume void fraction. Figure 2.1 (b) has shown the injectors setup. In our experiments we have used 1X2 where the number of injectors were 2, 2X2 where the number of injectors were 4, and 4X4 where the number of injectors were 16. In our experiments our bubble diameter varies from 4.1 to 4.9 mm. the corresponding Reynolds number is about 1200 and Weber number and Eotvos numbers are approximately 1.24 and 3.80. These non-dimensional numbers confirmed that the rising bubbles are oblate ellipsoid are in shape. We were aware enough to make enough space from the gas injectors to the wall to make the plume oscillates well in

the specific conditions. We have also visualized the bubble plume oscillation by the shadowgraphy image technique.

To perform the mixing characterizing experiment we have made an in-house low diffusive buoyant dye by using green food color, water and small amount of ethyl alcohol (to make the dye buoyant). To ensure the exact amount of dye for each experimental cases we have used a pump injector which can be seen in figure 2.2 (b). By using this the dye flow rate and the amount has controlled exactly same over the all experimental cases. In figure 2.2(a), the flow line for the dye has been showed. The dye has injected through two spargers, which can be shown in figure 2.2 (c). Our aim was to rest the liquid flow undisturbed so that the dye movement can be represented as bubble induced liquid flow. So that we have installed a flow line on the inner side of the column wall and make it unmovable over the experiment time. The results will be discussed in the results section.

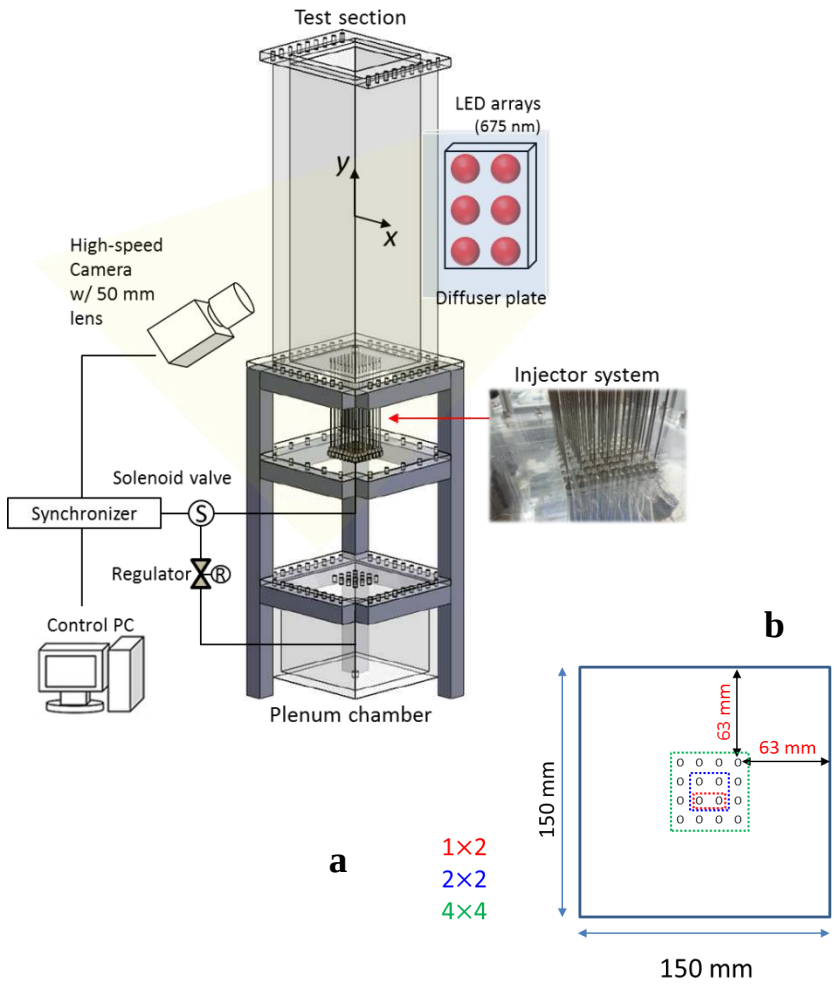

Figure 2.1: (a) Experimental setup for shadowgraphy image technique contains main bubble column with the high speed camera and LED arrays. (b) Three different (1x2, 2x2, 4x4) injectors setup for the experiments.

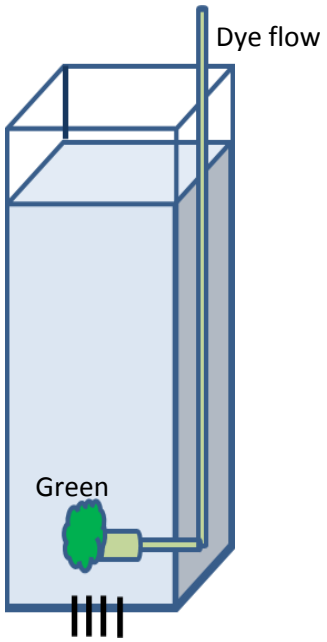

a

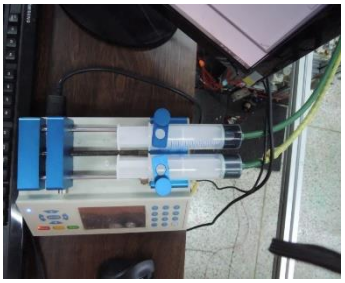

Injection pump

b

Spargers for dye injection

c

Figure 2.2: (a) Dye visualization experimental setup for mixing time experiments. (b) Injection pump. (c) Sprgers for dye injections.

Chapter 3

Image Processing Technique

Image processing technique has divided into two different steps. First one shadowgraphy image technique has performed to determine the bubble diameter. In the second phase we have processed the color image which has taken with a color ccd camera.

In the figure 3.1(a) the image processing technique has been showed to understand the procedure. After acquiring the raw image the initial binarization has been done and then filling & noise removal function has been applied. From Lau et al. (2013) we have applied bubble shape factor Ro which led us to get two distinctive image of 1) solitaire bubbles and 2) coalesced bubbles

After acquiring the coalesced bubbles image we have applied watershed technique to split the coalesced bubbles into single bubbles. Finally we added the watershed applied image with the solitaire bubbles and get the final images for performing PTV technique. The shape factor Ro can be described as –

$$Ro = \frac{P}{\sqrt{4\pi A}}$$

Here, P described as perimeter and A is the area of the bubble.

In figure 3.2 (b), (c), (d), a raw image, a binarized image and watershed applied image can be seen more precisely.

In figure 3.2 a color image processing has shown. At first we took a background image which is the water filled bubble column image without the bubbles. Then we have injected dye and triggered our bubble column. After that we have taken images. These raw images then subtracted from the raw image. With this we can neglect the noise and the subtracted image given us only dye contributed image. Later we have divided the subtracted image into red channel, green channel and blue channel. As our dye is green in color we have only considered green channel for our further calculation. Then we have applied Otsu method to find out the minima of our bubbles and extracted the bubbles from the every channel. Later we have reconstructed the image with combining red green and blue channel. This reconstructed image given us final image without bubble. Finally we again divided the image into three channel of red green and blue. And considered only green channel for our final concentration calculation. The whole process can be seen in figure 3.2.

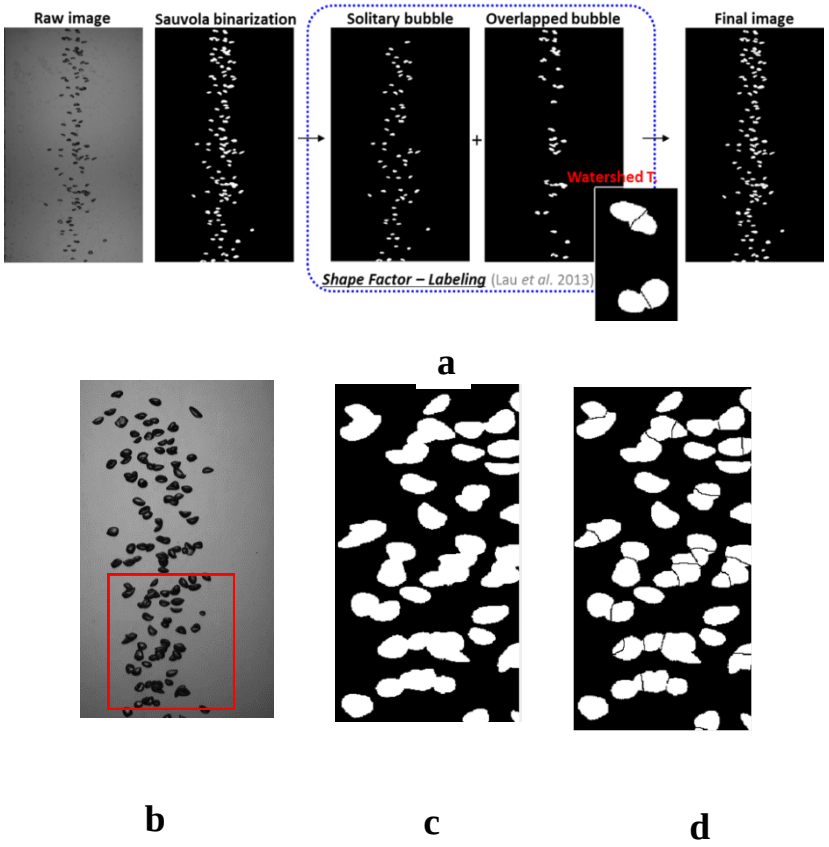

Figure 3.1: (a) Image processing steps for shadowgraphy image technique for calculating bubble diameter, bubble phase velocity, bubble size distribution etc. (b) A raw image. (c) Binarized image. (d) Watershed applied image.

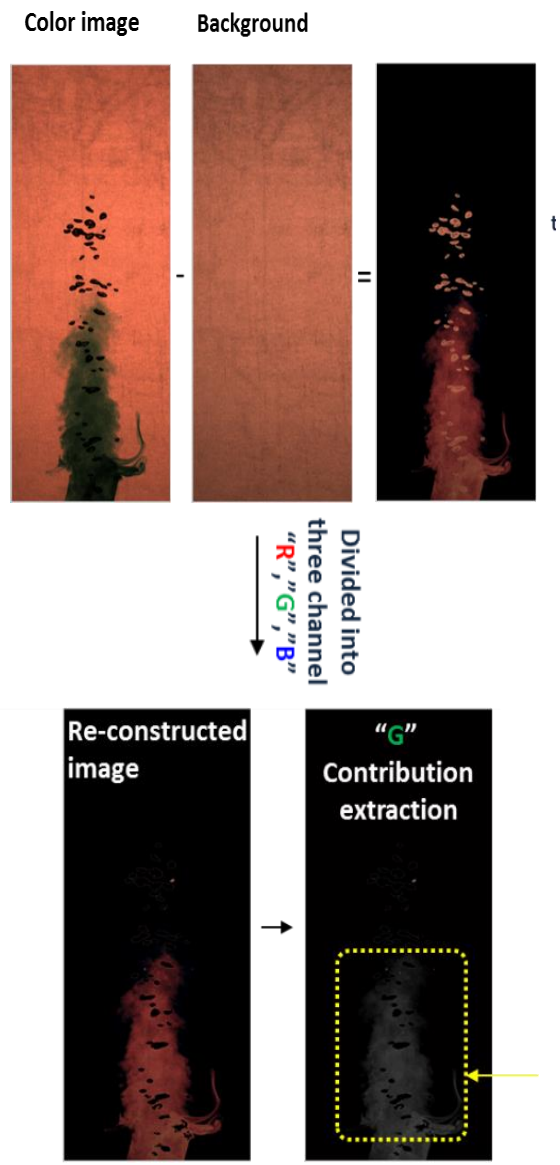

Fig 3.2: Color image processing steps and method for Dye visualized image.

Chapter 04

Results and Discussion

In the previous chapter we have said that for our experiments we have used three different injectors setup. And for those three injectors setup we have applied four different void fraction case for each experimental condition. So the total 12 experimental conditions has been tested. In the table 1, we can see all the 12 cases. From the table it can be seen that the aspect ratio has maintained for all the cases. The bubble rising velocity was in the range of 367 to 465mm/s. the diameter of the bubble were in the range of 4.1 to 4.9mm.

Bubble aspect ratio has calculated with the following method.

$$AR = \frac{major\ axis}{minor\ axis}$$

Bubble equivalent diameter has been calculated with the following method.

$$d_b = \sqrt[3]{a^2 b}$$

From the figure 4.1 (a) and (b) the pdf of bubble equivalent diameter and bubble rising velocity can be seen. From the pdf we can say that for all the cases mean values has maintained. Also it can be seen that the Gaussian profile has maintained for all the cases.

As far we have experimented 12 cases. But for our further analysis we have chosen only three cases to discuss our result. For 1x2 cases we have chosen the volume void fraction case of (α) = 0.010% here the number of injectors were 2 and

then 2x2 cases here the number of injectors were 4 and the volume void fraction was (α) = 0.020% and finally 4x4 cases here the volume void fraction was (α) = 0.075%. Interestingly we can see when the number of injectors were 2 the void fraction was 0.010 and when we doubled the injectors number, the void fraction also doubled in number and finally when we increased the injectors number the volume void fraction also get four times in number which is 0.075%. So it will be well enough to show this three cases for further analysis.

In figure 4.2 two instantons image has presented where we can see at the higher level of gas volume void fraction (0.075%) the bubble plume oscillates distinctively. This phenomena will be considered for describe other results as well.

In figure 4.3 it has clearly seen that the peak of volume void fraction measured highest for the upper void fraction case and lowest for the lower void fraction case. On the other hand it can be also said that the small number of injectors give us lower void fraction peak. Also for all the cases the highest peak has measured at the center. Also for lower elevation point in the bubble column void fraction compacted in the central region of the column and highest in number and for the upper elevation point in the column void fraction spreads and peak gets lower. This saturation effect was firstly investigated by the Rensen and Roig for their 2D bubble plume where they have mentioned that the bubble plume structure is clearly coupled with large scale recirculation and small scale eddies which all together created the plume boundaries and travel upwards. Benjan et al 1982 had modeled this phenomenon for single phase turbulent buoyant plumes. They stated that those large eddies coupled with the vorticity due mainly to the transversal gradient of the liquid velocity, are also partially responsible for the entrainment which is needed to supply the spreading of the liquid velocity profile.

In the figure 4.4 bubble rising velocity for the three cases has ploted. Here from the time averaged bubble rise velocity figure we can distinguish that in the core region highest bubble velocity occurs. Also at the inlet region bubble velocity is lower than the higher elevation point.

At the higher elevation point bubble rising velocity higher which is a cause of buoyancy and tendency of bubble to reach it's terminal velocity. Also, for 4x4 case bubble rising velocity is higher than other two cases.

In the figure it can be seen that the larger the void fraction the stronger the plume oscillation and this is also reflected in the spreading of the average velocity profiles. Stronger plume oscillations made the velocity profile broader and flatter. One thing we can say here that the evident roles of the oscillations in spreading the in time averaged plots, made the representation of any time-averaged computational profiles challenging. The bubble rising velocity shows Gaussian profile while at higher elevation the plume reaches at higher centerline velocity and a smoother edge.

Now let's consider the mixing experiments for the discussion. As in the previous section it is stated that a buoyant dye has used to visualize the liquid circulation and liquid structures as a method of direct visualization.

In figurre 4.4 we have attached three image from left to right contains α = 0.010%, 0.020%, 0.075% for a time t=0.5s. conting of time has started from the triggering of the bubble column. It is visible that the dye upward movement is faster for higher void fraction case than the lower void fraction case. As the dye is neutrally buoyant with the liquid (water). So the dye movement and structures can be represented with the liquid structures and movement. So for lower void fraction liquid rising velocity is lower than the higher void fraction case. Also bubble rising velocity is higher for higher void fraction case and bubble rising velocity is lower for lower void fraction case. So we can say that when the bubble rising velocity is higher liquid rising velocity is also gets higher and when bubble rising velocity is lower liquid risisng velocity is also lower (M.Simiano et al 2006, D. Colombet et al. 2015).

In figure 4.5 a series of liquid rising structures has shown for 2x2 case (α = 0.020%). Generally we can say from that figure in air water dye has transported over upward and then reaches at the top of the column after that spreaded over the surface of the water before following the liquid recirculation along the wall. One of thing for the first time we were able to see this type direct liquid structures. In spite of

numerous theoretical and experimental investigations in recent decades the flow patterns prevailing in bubble columns are still relatively poorly understood and difficult to predict (R.K. Upadhyay et al. 2013). So we hope this type of direct visualization will be helpful to develop further mathematical modeling.

With this direct visualization we later find out the mixing time for each cases. Mixing time has defined by the concentration profile. When the whole column concentration reached to the equilibrium then we say that it is fully mixed and that time has marked as mixing time.

More specifically, after injecting dye we triggered our bubble generator and on the same time we also triggered our color ccd camera. And take a series of photos of 0.5s intervals. As our main intention was to find out the mixing time and see the large scale circulations with liquid structures, we think 0.5s intervals were enough logical to proceed our experiments.

In the 4.6 figure we can see the concentration profile. From the left the first figure shows us the concentration profile for 1x2 and t = 6.5s. We can see that the normalized concentration profile, where $C_0$is the instantaneous pixel concentration and C_l is the initial dye concentration showed us that in the core region the dye or hereby we can say liquid is going upwards whether the other region are in rest and no circulation is not visible so far. But for 2x2 case (at the middle) concentration of green dye can be observed in all the region of the column though the profile is not stable. But at the last figure which is 4x4 we can say it has reached almost at the equilibrium. So with the void fraction mixing time also gets lower and the efficiency of bubble column also gets higher.

It will be interesting to show the relation between the void fraction and mixing time. Almeras et al. 2016 showed us that mixing time maintains a relation of $\frac{1}{\sqrt{\alpha}}$ with the void fraction. Though they conducted their experiments for the void fraction range of 1~3%. But in our case our gas volume void fraction are much lower than them. It is between 0.010~0.075%.

In the figure 4.7 we have plotted it and find out that our experiments also follows the same relation between gas volume void fraction. We have compared ou result with almeras et al 2016, 2014 and bouche et al 2013. Interestingly our experimental result falls in the same equation with them.

Nozzle	1 × 2				2 × 2				4 × 4			
	0.006	0.010	0.012	0.014	0.010	0.016	0.020	0.025	0.028	0.040	0.060	0.075
d_B	4.1	4.1	4.2	5.0	4.0	4.1	4.43	5.2	3.6	4.3	4.8	4.9
AR	1.9	1.9	1.9	1.9	1.8	1.8	1.8	1.8	1.8	1.8	1.8	1.8
V_B	367	378	385	425	355	405	424	439	384	433	445	465

a

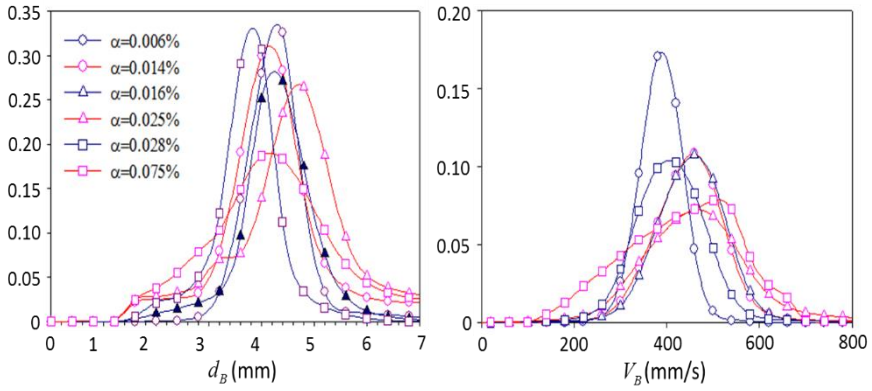

a **b**

Table 1: 12 experimental cases hydrodynamics Properties.

Figure 4.1: (a) PDF of Bubble equivalent diameter, (b) PDF of bubble velocity

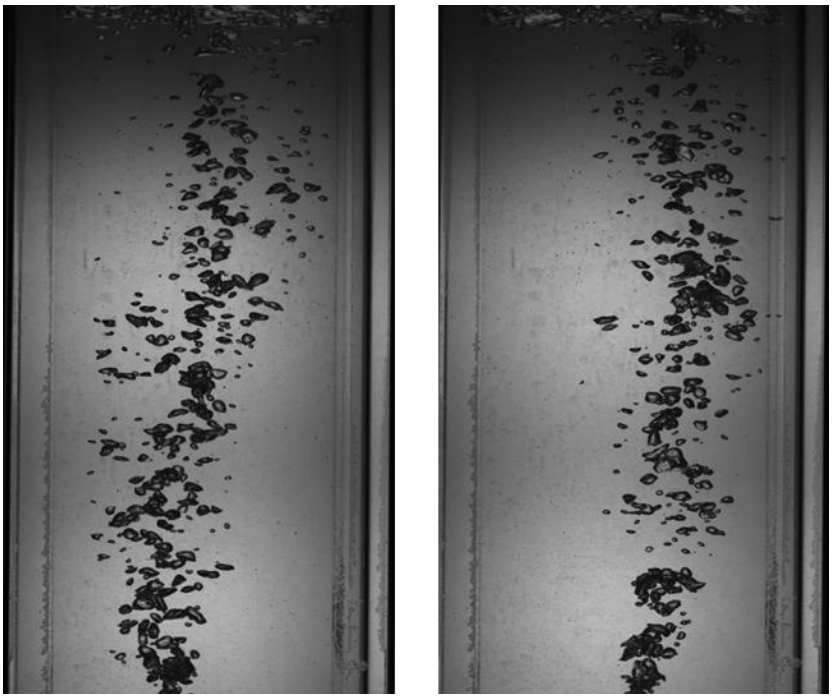

Figure 4.2: Bubble plume oscillation for the 4x4 (volume void fraction 0.075%)

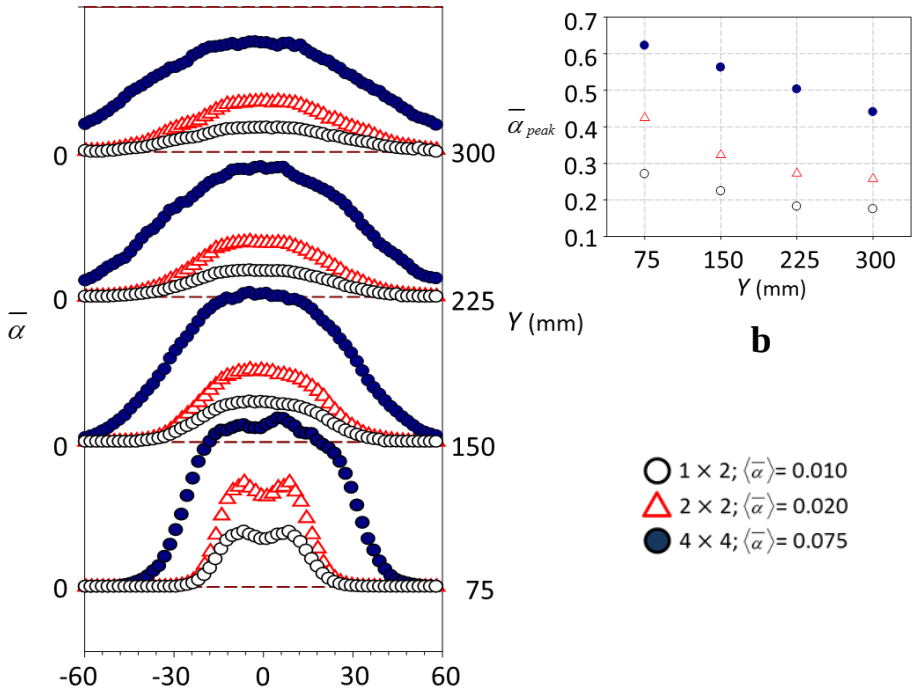

Figure 4.3: (a) Void fraction distribution for different longitudinal heights for three different cases. (b) Peak position of the void fraction for three different

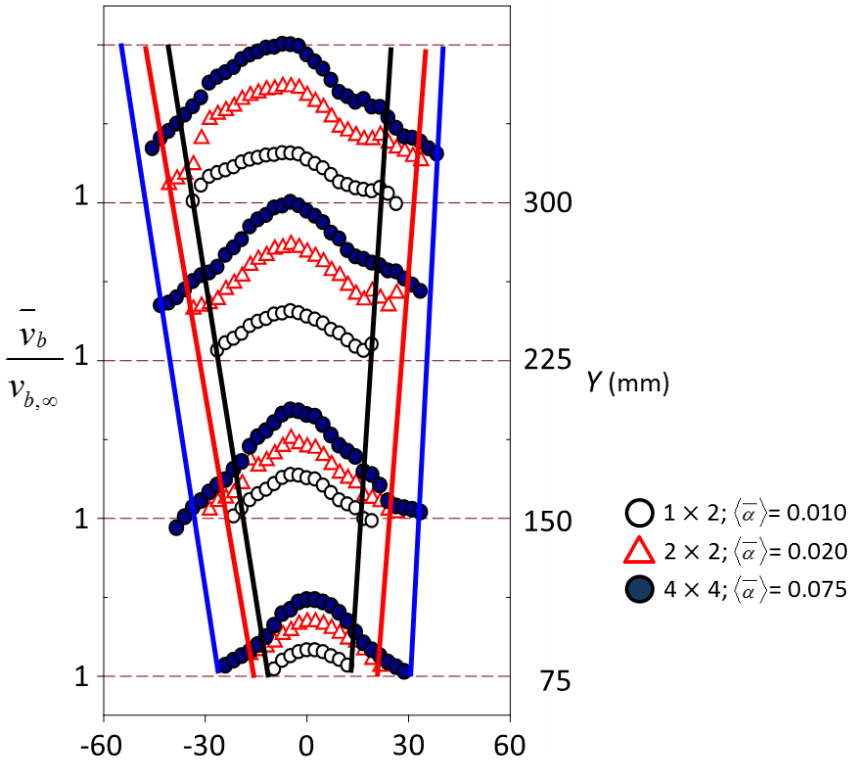

Figure 4.4: Normalized Bubble uprising velocity distribution for different longitudinal heights for three different cases.

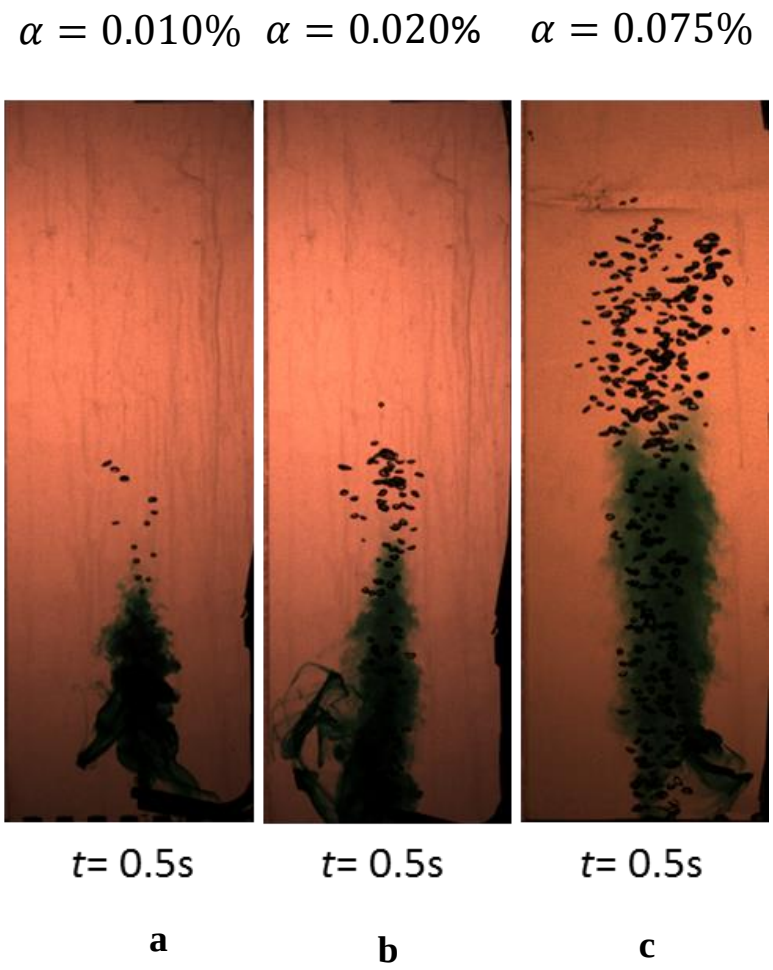

Figure 4.5: Dye visualized liquid structure for uprising liquid motion for three different case at a time of 0.5s. (a) $\alpha = 0.010\%$. (b) 0.020%. (c) 0.075%

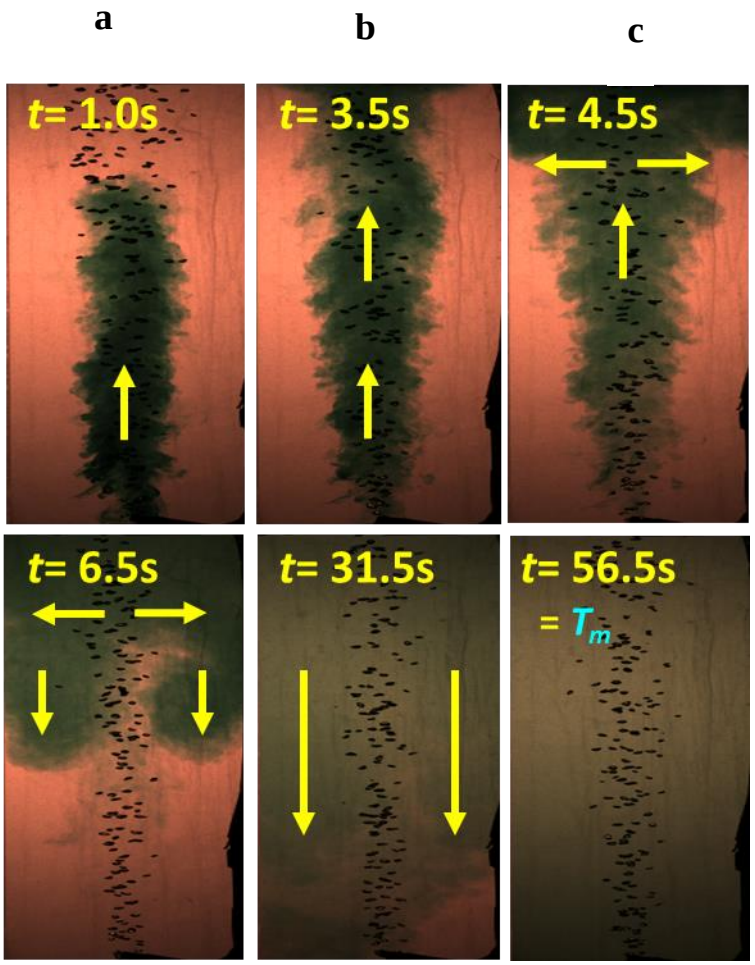

Figure 4.6: Dye visualized liquid structure for uprising and downcoming liquid motion for different time slab

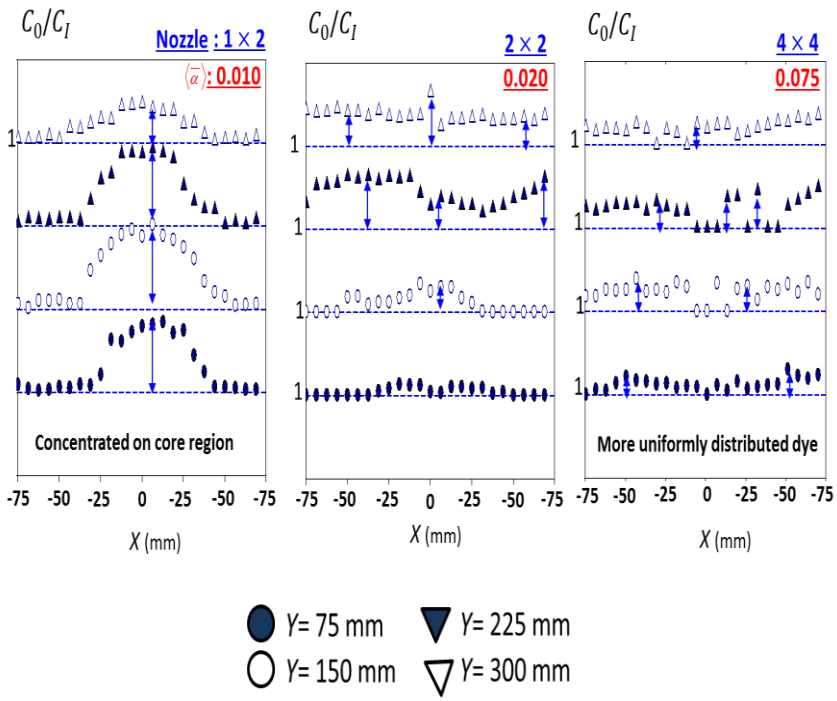

Figure 4.7: Concentration profile for green dye (a) 1x2, (b) 2x2, (c) 4x4 for a given time of t= 6.5s

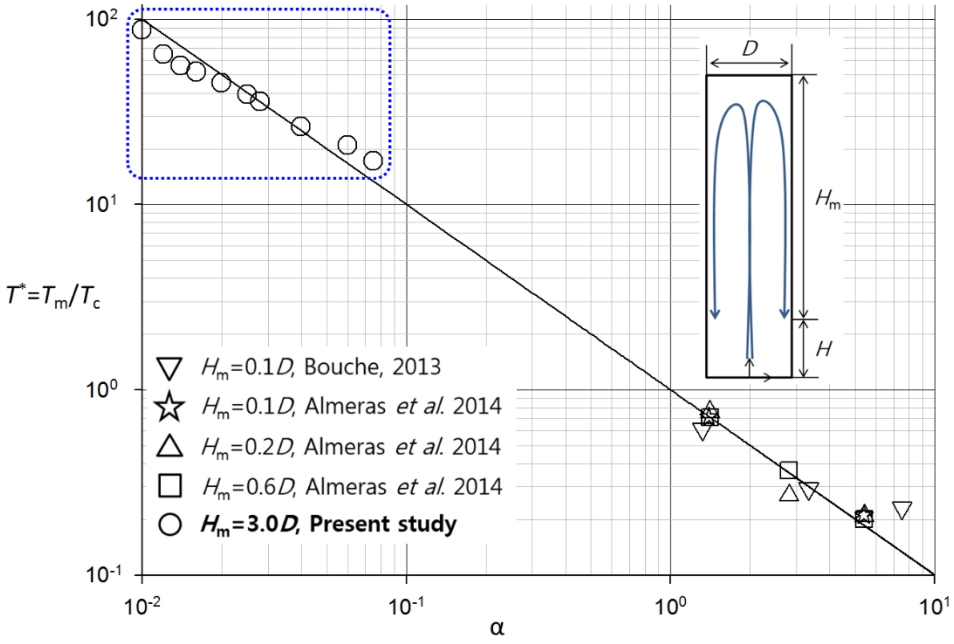

Figure 4.8: Relation between mixing time and volume void fraction

Chapter 5

Conclusion

In the present study we have so far showed an appropriate image processing method for finding out the basic properties for two phase bubbly flow. Later we have also developed the color image processing method for the direct visualization. Mixing of passive scalar has been investigated experimentally with the help of a dye.

In our present study we have so far investigated the fundamental hydrodynamics of the bubble column and validated the data with the theoretical and computational group as well with the previous experimental data. Based on that we have analyzed the mixing characteristics in a bubble column. In our experiments we have also showed the plume oscillation behavior in a bubble column. Though we think a lot of work like bubble bubble interaction, shear induced turbulence, wall effects, bubble induced turbulence those type of small scale calculation is also needed to carry out in future and an appropriate model is also important to predict the mixing characteristics.

The process we have applied for the mixing characterization is a direct dye visualization method. With this so far we can just reveal the large scale structure and the behavior. For the small scale structures we need to adopt the other experimental method like PIV. The turbulence properties analysis can be

another interesting part to show the mixing behavior in a bubble column. Continuous work on this issue will be continued on upcoming days.

Bibliography

(1) Alam, M., Arakeri, V.H., 1993. Observations on transition in plane bubble plumes. J. Fluid Mech. 254, 363-374.

(2) Almeras E, Risso, F.Roig, 2015. Mixing by bubble induced turbulence. J. Fluid Mech.776,458–474.

(3) AlmérasE.,Risso,F.,Roig,V.,Cazin,S.,Plais,C.,Augier,F.,2015.Mixingbybubble- induced turbulence.J.FluidMech.776,458–474.

(4) Batchelor, G.K 1967 An introduction to Fluid Dynamics. Cambridge: Cambridge University Press.

(5) E. Almeras, C. Plais, F. Euzent, F. Risso, V. Roig, F. Augier., Scalar mixing in bubbly flows: Experimental investigation and diffusivity modelling. Chemical Engineering Science, 140, 114-122.

(6) Freedman, W., Davidson, J.F., 1969. Holdup and liquid circulation in bubble columns. T 251Trans. Inst. Chem. Eng., T 25147, T 251.

(7) Iguchi, M., Okita, K., Nakatani, T., Kasai, N., 1997. Structure of turbulent round bubbling jet generated by premixed gas and liquid injection. Int. J. Multiphase Flow 23, 249-262.

(8) J. Rensen, V. Roig, 2001, Experimental study of the unsteady structure of a confined bubble plume. Int. J. Multiph. Flow. 27, (1431-1449).

(9) Law, Y. M., Deen, N. G. and Kuipers, J. A. M., 2013, Development of an image measurement technique for size distribution in dense bubbly flows, Chem. Eng. Sci., Vol. 94, pp. 20~29.

(10) M. Simiano, R. Zboray, F. de Cachard, D. Lakehal, G. Yadigaroglu, 2006, Comprehensive experimental investigation of the hydrodynamics of large-scale, 3D, oscillating bubble plumes, Int. J. Multph. Flow. 32, 1160-1181.

(11) Nigar Kantarci, Fahir Borak, 2005, Review on Bubble Column Reactors, Process Biochemistry 40(2005) 2263-2283.

(12) Rajesh K. Upadhya, Harish J. Plant, Shantanu Roy, 2013, Liquid flow pattern in rectangular air water bubble column investigated with radioactive particle tracking. Chemical Engineering Science 96, 152-164.

(13) Zhengliang Liu, Ying Zheng, Lufei Jia, Qikai Zhang, 2005, Study of bubble induced flow structure using PIV. Chem. Eng. Sci. 60, 3537-3552.

사각 기포탑 혼합 및 수력학적 특성에 관한 실험적 연구

서울대학교 대학원

기계항공공학부

자히둘

요약

본 연구에서는 고속카메라를 이용하여 획득한 이미지를 대상으로 앞서 수행한 이미지처리 알고리즘을 동일하게 적용하여 기포분포 및 거동을 측정하였다. 그림 13a 은 총 64 개의 노즐 중, 정방형으로 놓인 가운데 16 개(4×4)의 노즐을 선택적으로 사용하고 이를 개별적으로 조절하여 얻은 이미지 및 이미지처리 최종 결과이다. 기포 및 기포탑에 의한 혼합효과를 파악하고 이를 정량화시키기 위해선 먼저 높이에 따른 기포들의 분포를 파악하고, 기포분율 증가에 따른 기포탑의 수력학적 특성을 파악해야한다. 이를 위해 본 연구에서는 노즐 당 유량을 일정하게 유지한 채, 노즐 개수 4 개(2×2)와 16 개(4×4)에서 발생되는 부피분율이 각각 약 2%와 8%에서 높이에 따른 local void fraction 및 instantaneous positioning of the plume 을 분석하였다.

부력에 의해 중앙에서 상승하는 기포탑유동은 다양한 scale 의 액체유동을 유발하는데, 그중 대표적인 large-scale 유동으로 기포탑과 벽면사이에서 발생되는 liquid circulation 이 있다. 본 연구과제에서는 기존의 문헌을 참조하여 벽면효과를 배제시키기 위해 한변의 길이가 150 mm 인 사각관을 제작하였고, 오직 기포탑에 의한 생성된 liquid circulation 이 수면에서부터 노즐입구로 내려오며 발생시키는 instability 를 관찰하였다. Instability 에 도달한 기포탑의 비정상유동을 관찰하는것 뿐만 아니라, 각 부피분율에서 기포탑이 진폭을 갖지 않고 수직상승하는 비교적 단순한 기포탑유동에 대한 시간평균된 기포의 거동을 분석하였다. 그림 14 를 통해 확인 할 수 있듯, 서로 다른 부피분율을 갖는 기포탑 정상유동은 공통적으로 높이에 따라 폭이 넓어지고, 확산되는 것을 확인 할 수 있다.